A SPATIOTEMPORAL MODEL TO SIMULATE CHEMOTHERAPY REGIMENS FOR HETEROGENEOUS BLADDER CANCER METASTASES TO THE LUNG

KIMBERLY R. KANIGEL WINNER[1,2], JAMES C. COSTELLO[1,2,3]

[1]Computational Bioscience Program,
[2]Department of Pharmacology,
[3]Univeristy of Colorado Cancer Center
University of Colorado Anschutz Medical Campus
12801 E. 17th Ave. MailStop 8303,
Aurora, CO 80045, USA
Email: kimberly.kanigelwinner@ucdenver.edu, james.costello@ucdenver.edu

Tumors are composed of heterogeneous populations of cells. Somatic genetic aberrations are one form of heterogeneity that allows clonal cells to adapt to chemotherapeutic stress, thus providing a path for resistance to arise. *In silico* modeling of tumors provides a platform for rapid, quantitative experiments to inexpensively study how compositional heterogeneity contributes to drug resistance. Accordingly, we have built a spatiotemporal model of a lung metastasis originating from a primary bladder tumor, incorporating *in vivo* drug concentrations of first-line chemotherapy, resistance data from bladder cancer cell lines, vascular density of lung metastases, and gains in resistance in cells that survive chemotherapy. In metastatic bladder cancer, a first-line drug regimen includes six cycles of gemcitabine plus cisplatin (GC) delivered simultaneously on day 1, and gemcitabine on day 8 in each 21-day cycle. The interaction between gemcitabine and cisplatin has been shown to be synergistic *in vitro*, and results in better outcomes in patients. Our model shows that during simulated treatment with this regimen, GC synergy does begin to kill cells that are more resistant to cisplatin, but repopulation by resistant cells occurs. Post-regimen populations are mixtures of the original, seeded resistant clones, and/or new clones that have gained resistance to cisplatin, gemcitabine, or both drugs. The emergence of a tumor with increased resistance is qualitatively consistent with the five-year survival of 6.8% for patients with metastatic transitional cell carcinoma of the urinary bladder treated with a GC regimen. The model can be further used to explore the parameter space for clinically relevant variables, including the timing of drug delivery to optimize cell death, and patient-specific data such as vascular density, rates of resistance gain, disease progression, and molecular profiles, and can be expanded for data on toxicity. The model is specific to bladder cancer, which has not previously been modeled in this context, but can be adapted to represent other cancers.

1. Introduction

1.1. *Tumor heterogeneity and drug resistance*

Intratumoral heterogeneity is increasingly recognized as a major contributor to cancer progression, metastatic potential, and drug resistance.[1,2] Metastatic tumors that arise from the primary site are generally established from single clones, but may also display initial genetic heterogeneity.[3,4,5] Sub-clonal cell phenotypes with varying metastatic potential and drug resistance have also been shown to develop in 90% of lung metastases within weeks of establishment in mice.[5] This heterogeneity can lead to differential drug response within or among metastases, with newly arising clones developing additional resistance.[5] After the death of sensitive cells and continuing replication of resistant survivors, the spatial dynamics of drug diffusion and accumulation during later drug delivery cycles may change.

A bottleneck in clinical research studies of drug resistance is the lack of tumor sample measurements over the course of treatment from the same patient that can be used to explore the relationship between tumor polyclonality and drug resistance.[6] By building explicit computational

models with evolving dynamics, we can manipulate, visualize, and quantitatively analyze patterns of resistance that emerge in a growing tumor. Here, we have created a spatiotemporal model of bladder cancer metastasis to the lung that includes cycles of drug delivery, tumor vascularity, and clumped clonal populations with different drug sensitivities. We model how a heterogeneous tumor responds to the standard first-line regimen of gemcitabine plus cisplatin (GC). Results show that a 100 cell simulated tumor, composed of four clonal populations ranging from highly sensitive to highly resistant cells will not be completely killed by this regimen, and will grow while gaining cross-resistance to both gemcitabine and cisplatin. In this work we aim to model drug response in bladder cancer metastases and establish a baseline set of results that can be extended to model additional visceral sites, determine how varying tumor composition affects drug response, and determine how altering drug scheduling will affect drug response.

1.2. *Prior spatiotemporal models of drug delivery, tumor heterogeneity, and resistance*

Our model is a cellular Potts model, which represents cells and chemical fields on a spatial lattice, interacting and evolving over time. Spatiotemporal models have been used to represent disease development and drug delivery in a variety of cancers, and have generated observations that are not easy to measure in real biological systems.[7–9] They have incorporated parameters such as response to oxygen, information sources provided to the cell such as nutrients and toxicity, and distance from the information source.[8] Spatiotemporal cancer therapy models have used cell cycle, chemotherapy, and radiation data to predict changes in tumor size during treatment. Some have included more specialized events and data, such as bystander effects (in which tumor cells assist in killing damaged cells) resulting from radiotherapy[10] and patient data from CT scans in models of brain cancer.[11,12] These models have successfully produced qualitatively and semi-quantitatively comparable results to *in vitro* studies*,* mouse models, and patient outcomes, showing the promise of spatiotemporal modeling for *in silico* oncology. To our knowledge, there are no existing spatiotemporal models of drug delivery to lung metastases arising from bladder cancer.

Tumor heterogeneity and resistance have been explored with spatiotemporal methods, including two agent-based models (one incorporating game theory for trade-offs between proliferation and migration), field theory, a cellular automaton/cellular Potts model, and a pure cellular automaton. Interestingly, in three of these models,[13,14,15] slowing of the cell cycle was an important predictor of resistance, whether due to cells being driven into quiescence by drugs, by a shortage of oxygen and nutrients, or from initial heterogeneity between clonal populations in their endogenous cell cycles; cells with inherently slow growth were reservoirs for survival during therapies that depend on cell division.[14,15] This last model is the most similar to ours, and is part of a comparison of spatiotemporal implementations, showing that there are trade-offs between performance and resolution for different model types, but that similar types parameterized to the same system will produce cross-validating results. The simulated tumor in ref. 15 was composed of cell populations having heterogeneous cell cycles that changed in response to oxygen, chemotherapy, and radiation (in a 300×300 cellular Potts model). Our model similarly includes cell cycles and chemotherapy, but is different in that it creates a site-specific tumor environment incorporating vascular density specific to metastases to the lung, with *in vivo* concentration curves for drug delivery, and initial and gained resistance modeled using bladder cancer cell lines. In both

models, the spatial arrangement of vessels creates a drug concentration unique to each cell in a simulation, allowing spatially driven phenomena to emerge.

1.3. *Bladder cancer drug regimen and cell response*

Annually, it is estimated that there will be nearly 77,000 new cases of bladder cancer with over 16,000 succumbing to the disease.[16] Overall survival has not improved since 1989.[16] The most aggressive form, muscle-invasive bladder cancer, occurs in 30% of patients.[17] Treatment is radical cystectomy, requiring removal of the bladder and sometimes surrounding tissues, followed by chemotherapy. The 5-year survival rate varies from 25-50%. Failure is likely due to occult metastases present before treatment, with the most common visceral metastatic sites in the liver and lungs.[17,18] Patients with inoperable locally advanced or metastatic cancer who undergo GC or methotrexate/vinblastine/doxorubicin/cisplatin (MVAC) regimens have a 5-year overall survival of 13%, but a progression-free survival of 9.8%.[19] Those with lung, liver, or bone[18] metastases have a 5-year overall survival rate of 6.8%.[19] Here, we model this last group of patients, with aggressive metastatic disease localized to the lung.

The standard regimen defined by the National Comprehensive Cancer Network (NCCN) for metastatic bladder cancer includes six 21-day cycles, with GC delivered simultaneously on day 1 (or cisplatin instead on day 2) and gemcitabine alone on day 8.[20] For patients with muscle-invasive or metastatic cancer, who cannot receive cisplatin, monotherapy regimens without cisplatin produce no long-term disease-free survival, with a median survival of six to nine months.[17] This was reflected in initial runs of the model, with rapid acquisition of resistance during cisplatin or gemcitabine monotherapy regimens. Reported efficacy of such regimens is derived from clinical trials. Computational models of drug delivery can additionally be used to generate hypotheses at a small scale where we can explore mechanisms of drug action and drug resistance, as well as adjust the regimen in a consequence-free environment where results for 18 weeks of time course data can be obtained in just hours.

Cisplatin and gemcitabine are genotoxic agents, damaging DNA and causing a cell to undergo apoptosis during cell division. Cisplatin incorporates into DNA as platinum-DNA adducts,[21] whereas gemcitabine is a nucleoside analog that interrupts DNA synthesis and triggers apoptosis.[22] The 50% inhibitory concentration (IC50) is a concentration of drug that inhibits a cellular process by 50%. IC50 for cytotoxicity and drug accumulation in cells are linearly correlated for both cisplatin and gemcitabine, especially at clinically relevant concentrations, which tend to be at the lower end of cytotoxicities measured *in vitro*.[23–25] There is also a linear relationship between tissue platinum concentration and tumor size reduction.[26] These relationships were used to parameterize cellular accumulation of the two drugs.

Synergy between gemcitabine and cisplatin occurs during pre-treatment with gemcitabine or co-treatment with GC in ovarian and neuroblastoma cells.[27,28] In these studies, one in four and one in five cell lines did not respond synergistically. Patients with non-small-cell lung cancer also responded better to a day 1 combination of gemcitabine and cisplatin than to day 1 cisplatin alone (30.4% response compared to 11%, p<1e-4), with improved median time to progression and improved overall survival.[29] Synergy in cisplatin during the GC regimen is an important dynamic that we include in the model.

2. Methods

2.1. *Summary of model design*

Our model represents a partially drug-resistant lung metastasis that arose from a primary bladder tumor, containing four clonal cell patches with different sensitivities to gemcitabine and cisplatin. The drugs are delivered through vasculature in the tumor at levels found in patient plasma based on the regimen dosages. Drugs diffuse from vessels with effective diffusion coefficients measured in tumor tissue, and accumulation is a cell-type-specific proportion of drug concentration at the cell site. Synergy between the drugs causes increased intracellular cisplatin accumulation. If cells attempting to replicate have accumulated enough drug to reach their IC50 or greater, they will either die with 50% probability or increase their resistance. Finally, when a cell divides, its accumulated drug is halved between the two child cells. Drug delivery frequency and dosage are from the basic GC drug regimen for metastatic bladder cancer (see Fig. 1 for model).

Tumor and vessel cell types are represented, along with cell division, cell death, and clearance of dead cells as a proxy for the immune system. Vascular density for lung metastases is equal to the ratio of microvessel density between primary and lung metastases in non-clear cell renal cell carcinoma.[30,31] Further biometric parameters, derivations, fits for drug concentrations in patients, and their sources can be found in Table 1. Model permutations include runs with and without synergy, variations on the drug regimen, and variations in rates of resistance gain in the cells.

The modeling platform is Compucell3D (CC3D),[32] an integrated programming and visualization environment for cellular Potts models. Cellular Potts models couple mobile, single-cell agents to a cellular automaton process at the cells' surfaces. Cell agents live on their own 2-D or 3-D lattice, and chemical fields can be layered on in other lattices. Partial differential equations for drug diffusion are solved using the Forward Euler method. For more explicit descriptions of the cellular Potts model for modeling drug delivery in tumors, please see Kanigel Winner, et al.,[33] and Extended Methods are available at https://synapse.org/MetHet. In short, pre-defined biological rules comprise an energy function that drives the behavior of the cellular automaton process at the cell surface during each Monte Carlo time step (MCS). Meeting the rules (by convention) lowers this energy or keeps it the same, allowing biologically reasonable cellular events contributing to growth, division, and death (though stochasticity can be added). Cell death, cell type switches due to drug accumulation, and drug delivery calculated from continuous functions (fits to patient plasma drug concentrations) are expansions of the basic CC3D model coded in a Python wrapper. These processes are non-stochastic. More modeling methods, details of parameter acquisition, and source code that is plug-and-play in CC3D can be found at https://synapse.org/MetHet.

2.2. *Specifics of biological parameters and model dynamics*

- IC50 data for gemcitabine and cisplatin sensitivity in 18 bladder cancer cell lines were acquired from the Genomics of Drug Sensitivity in Cancer (GDSC) database.[34]
- Cell growth and division occurred in all cancer cells. Replication rate was approximated from the averages of 14 cancer cell lines varying in metastatic capacity (31 to 33 hrs.).[22,36,37]
- Cisplatin and gemcitabine in normal cells (lung and phagocytic cells) were given accumulation rates for the bladder cancer cell line (SW780) closest to the middle of the range for both drugs.
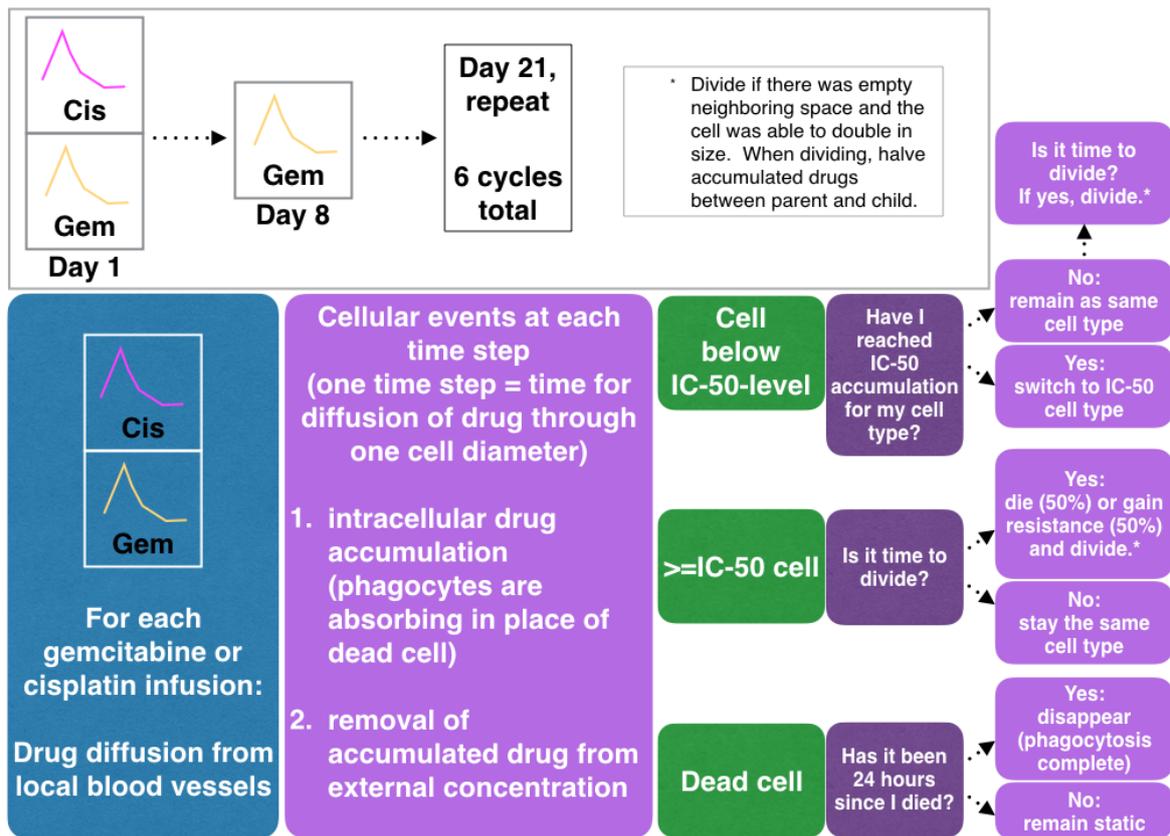
Figure 1. Flow chart of events in the model at each time step, reflecting body- and cellular-scale processes

- Acquired resistance was modeled as an increase in the IC50 of any cell that survived an IC50 accumulation of gemcitabine or cisplatin at division time, increasing the chances of being below IC50 and another gain in resistance at the next division time. The quantity to be added to the IC50 for each gain in resistance (Table 1) was derived from bladder cancer cell lines, passaged to increase resistance, as the increase per division required to acquire maximum resistance over one year ("quick") or two years ("slow") for cells with a 30-hour cell cycle.[35]

- Cell accumulation rate and peak of gemcitabine is linearly correlated with concentration *in vitro* and *in vivo*.[38] In bladder cancer cells, cytotoxicity is linearly correlated with gemcitabine concentration,[25] and accumulation is correlated with IC50.[36] Cisplatin DNA lesion counts are linearly correlated with concentration.[27] We therefore fit cellular accumulation rates for both gemcitabine and cisplatin linearly to the IC50 of each cell type, with some modifications.[36,39]

- Cells at IC50 for both gemcitabine and cisplatin at division underwent two chances at death.

- Gemcitabine and cisplatin were modeled with the same effective diffusion coefficient as sodium fluorescein.[40] For details on this choice, please see ref. 33. Both molecules diffused at the same rate in all cell types except for blood vessel, which either took away molecules, ostensibly into flowing blood, or delivered them from the vessel surface.

.

Table 1. Model parameters and fits to data

Parameter	Value	Units	Source
Cell diameter (BC[*] T24 line, aggressive/invasive)	30	μm	[42]
Eff. diffusion coefficient sodium fluorescein	6.40E-06	cm^2/s	[40]
Division time (mean, S.D.)	30, 1	h	[22,36,37]
Time from death to complete phagocytosis	24	h	[43]
Fraction cross-sectional microvessel area in metastasis from urinary system cancer to lung	0.146		[30]
Pixel dimension	1	cell	
Cisplatin resistance gain per survived division	0.125 – 0.25	+ IC50	[35]
Gemcitabine resistance gain per survived division	0.05 – 0.1	+ IC50	[35]
IC50 cis. accumulation for initial cell lines. Seed gem. & cis. sensitive, Seed res. gem./sens. cis., Seed res. cis./sens. gem., Seed gem. & cis. resistant	0.8106177157, 3.774888444, 6.586828431, 5.923917064	μM per cell	calculated using fit from [44]
IC50 gem. accumulation for initial cell lines. Seed gem. & cis. sensitive, Seed res. gem./sens. cis., Seed res. cis./sens. gem., Seed gem. & cis. resistant	0.000017923, 270.913928515, 0.145644144, 46.134163935	μM per cell	calculated using fit from [36]
Accumulation rates of cis. in initial cell lines. Seed gem. & cis. sensitive, Seed res. gem./sens. cis., Seed res. cis./sens. gem., Seed gem. & cis. resistant	7.98701E-05, 6.82909E-05, 7.42347E-06, 5.46716E-05	* cis. (μM) at cell site per MCS	fit from [44]
Accumulation rates of gem. in initial cell lines. Seed gem. & cis. sensitive, Seed res. gem./sens. cis., Seed res. cis./sens. gem., Seed gem. & cis. resistant	4.41575E-04, 2.68443E-04, 4.41518E-04, 4.22858E-04	* gem. (μM) at cell site per MCS	fit from [36]
Fit for cisplatin plasma concentrations during 3h infusion (top) and decay (bottom)	$= 0.11*hrs^3 - 0.83*hrs^2 + 2.2*hrs - 2.6E-16$ $= 57.4124 * e^{(-1.0927 * hrs)}$	μM	[46]
Fit for gemcitabine plasma concentrations during 30m infusion (top) and decay (bottom)	$= 6.8*(min/15 - 1) + 7.3$ $= 101.3452 * e^{(-0.0676 * min)}$	μM	[45]
Synergy multiplier for cisplatin accumulation	2.5		[27,28]
Total Monte Carlo (simulation) Steps (126 days)	11,916,800		
Time in one Monte Carlo Step (MCS)	0.914	s	

* Bladder Cancer

3. Results

3.1. *No standard or alternate regimen prevents regrowth of a drug resistant tumor*

In preliminary simulations containing only GC dual-sensitive cells, cells declined over time and the population was killed late on day 48, five days after the third round of GC. However, for an initial tumor with three additional cell types that had increased resistance to gemcitabine, cisplatin, or both, neither the standard GC regimen (Figs. 2,3), nor an unrealistically high rate of delivery of gemcitabine could kill all cells.

The initial 2-D tumor of 100 cells consistently quadrupled to 400 cells in 14 to 15 days. At simulation end, 0 to 18 days after the last round of drug (depending on the simulation) the domain was completely filled with drug-resistant tumor cells, primarily cisplatin-resistant and GC dual-resistant cells, as well as a sub-population of the most GC dual-resistant seed population. Within

six hours of regimen start, the two most sensitive cell types reached the IC50 for gemcitabine accumulation. While some of these sensitive cells died, some went on to propagate as sub-clones with gained resistance.
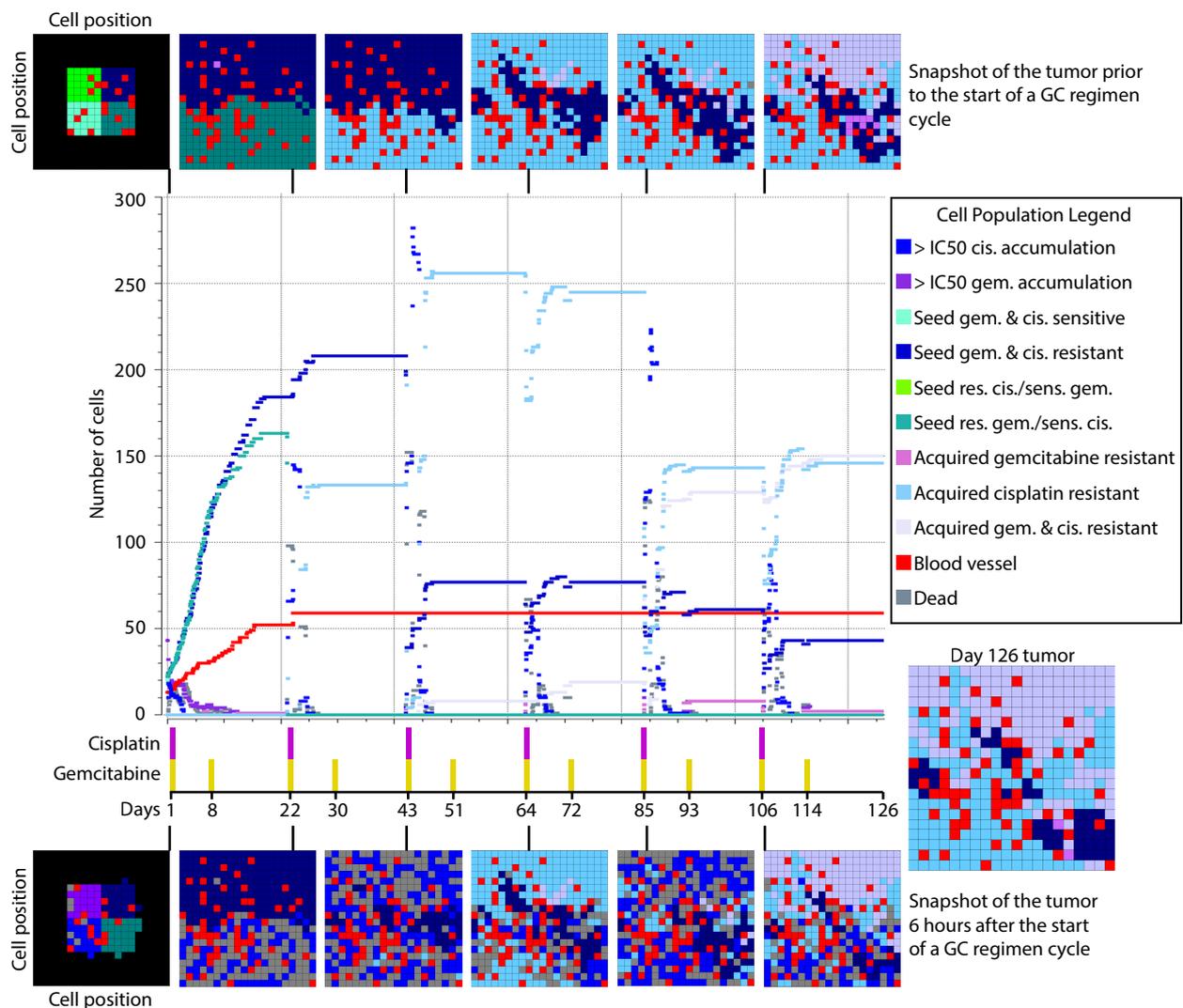

Figure 2. A simulation with random uniform "slow" to "quick" acquired resistance for all cells, and drug synergy in all cells. Pulses of gemcitabine and cisplatin or gemcitabine alone for the first-line chemotherapy regimen are displayed and matched to the simulation. Cells in the simulation were seeded in 100-cell tumors shown in the top-leftmost simulated tumor diagram. The row of simulated tumors on the top represent the state of the tumor before the start of a chemotherapy cycle; the row of simulated tumors on the bottom represent the state of the tumor 7 hours after a GC cycle. Resistant seed cells, cells with dual resistance, and cells with cisplatin resistance composed the final population as shown as the final simulated tumor after 126 days of treatment.

3.2. *Effects of acquired resistance*

3.2.1. *Ability of cells to gain resistance increases likelihood of dual resistance*

When acquired resistance was allowed to arise in the cell populations, cells with acquired resistance comprised the majority of the final tumor (Figs. 2, 3). GC dual-resistant sub-clones arose at day 43, after the third cycle of GC, suggesting that increased dosage or delivery rate prior

to this time point may help to keep cross-resistant strains from arising. Interestingly, the fastest rate of acquired resistance for both gemcitabine and cisplatin drove cells with acquired resistance to cisplatin to dominate the population.
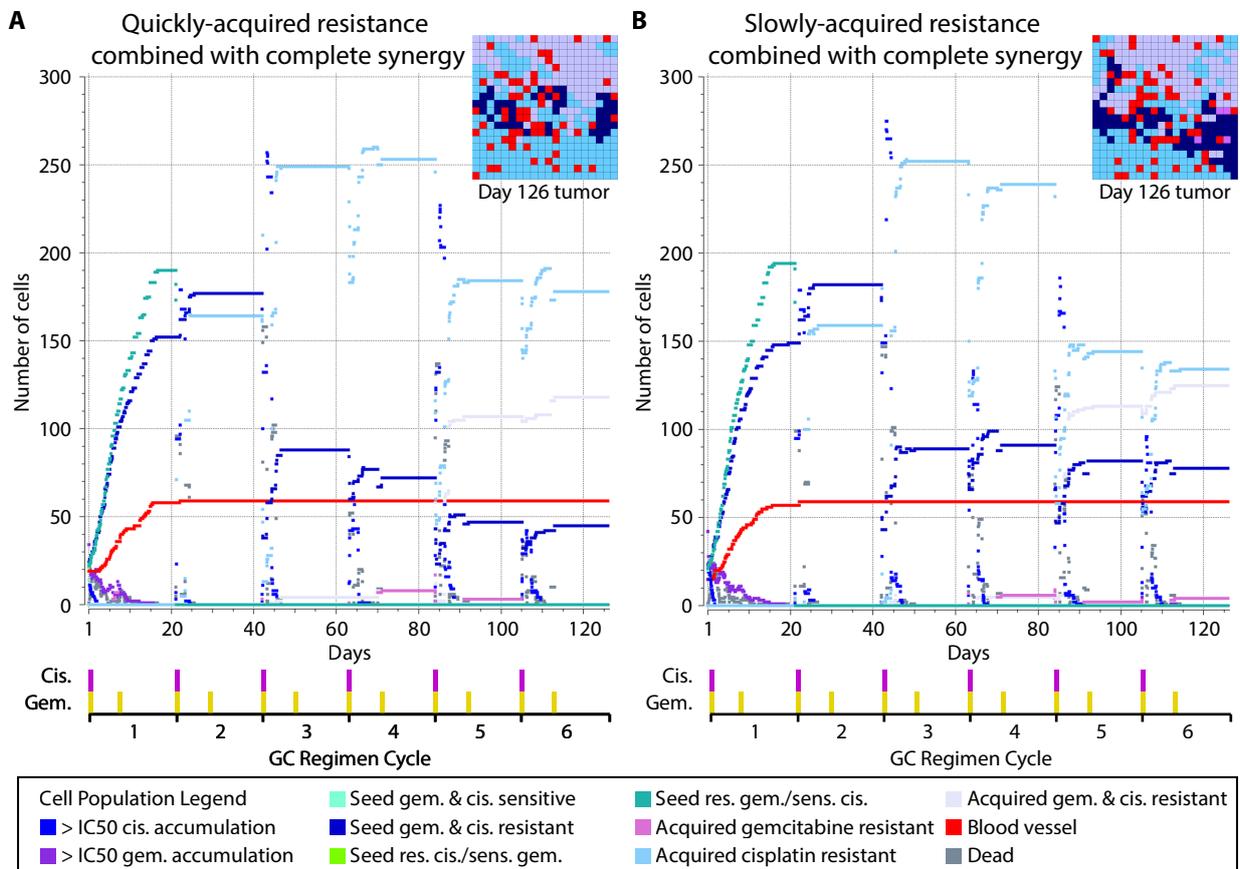

Figure 3. (A) Quickly-acquired resistance and (B) slowly-acquired resistance resulted in tumors composed primarily of cells with newly acquired resistance, with a smaller population of highly GC dual-resistant seed cells. Quickly-acquired resistance drove the tumor toward greater cisplatin resistance.

3.2.2. *Simulated tumors show complete resilience to even intense treatment*

In simulations with an added pulse of gemcitabine at day 18 during each cycle (we mirrored the timing of the 28-day regimen, which has an additional gemcitabine infusion on day 18), we found an earlier rise of the GC dual-resistant phenotype, and more gemcitabine-resistant cells. We also applied single-drug regimens with cisplatin or gemcitabine alone at standard frequencies. Cells with resistance to the treatment drug were the majority of the final population.

To try treatment prior to all cells entering a new cell cycle (30 hrs) while using a potentially tolerable regimen, we shifted the three pulses of gemcitabine to the first three days of each 21-day cycle, at every 24 hours, in addition to the standard cisplatin every 21 days. This caused the end state to be dominated by GC dual-resistant cells. Finally, we pulsed gemcitabine every 24 hours for 126 days, with cisplatin every 21 days. The tumor was not killed, and the simulated tumor

area was fully repopulated, primarily with cisplatin-resistant cells after 126 pulses of gemcitabine reduced the gemcitabine-resistant populations.
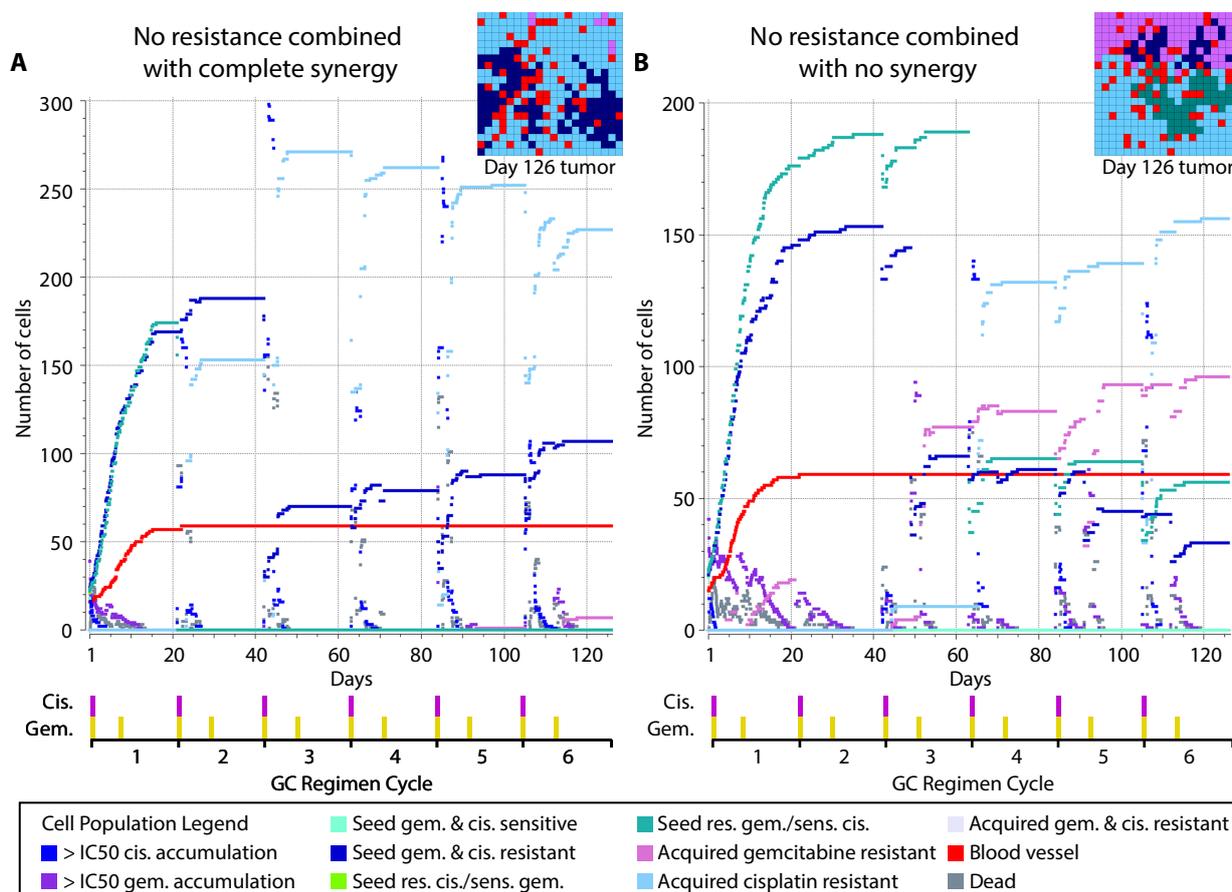

Figure 4. In simulations without acquired resistance, models were considered (A) with drug synergy between gemcitabine and cisplatin and (B) without synergy. The final tumor was composed of cells that survived division after reaching either cisplatin IC50 accumulation, or gemcitabine IC50 accumulation. Cells that survived both gemcitabine and cisplatin IC50 levels did not arise. When there was no synergy in cisplatin (2.5× normal accumulation rate, B), an extra cell type (teal-colored) derived from the seed populations remained.

3.3. *In the absence of acquired resistance, diffusion of drug via cell division allows survival*

In simulations where cells did not acquire resistance, populations primarily composed of cells that randomly survived an IC50-cisplatin division (Fig. 4A) repopulated the simulation space. A subpopulation of initial highly GC dual-resistant seed cells also survived. Because of the division of drug equally between two progeny cells, acquired resistance was not required for tumor repopulation, suggesting that cells reaching IC50 accumulation may survive *in vivo* without newly acquired resistance. In simulations with synergy and resistance (Figs. 2, 3), one clone in the original tumor died during the second round of GC at day 21 (teal-colored; $IC50_{cisplatin} = 14.0\mu M$ in range 2.6μM to 225.2μM). When synergy and the ability to gain resistance were absent, this cell type comprised a substantial portion of the final tumor, the most heterogeneous final tumor in our models (Fig. 4B). Hence, for the most resistant seed cells, and in less resistant seed cells in which synergy may not be active, no acquisition of extra resistance was required for repopulation.

4. Discussion

In this work, we were able to capture population-level responses to chemotherapy stress in a model of lung metastasis arising from the bladder. Unless the initial tumor was comprised of highly sensitive cells, the *in vivo* concentration and timing of the standard first-line regimen did not kill the metastasis. Cells were then able to proliferate and fill the simulation space after completion of treatment. A striking result was that in tumors without any ability to acquire resistance, some cells survived the IC50 threshold and were able to repopulate the space. When tumors were allowed to acquire resistance, there was consistent emergence of cells that had coordinately increased resistance to both gemcitabine and cisplatin around 43 days. This occurred after the third cycle of GC, suggesting that early aggressiveness in treatment may be important in avoiding cross-resistant sub-clones. In terms of drug-directed cell selection, when cells were given the ability to acquire resistance, even at slower rates described *in vitro*, final tumors were composed of a majority of cells with acquired resistance. Because metastases starting from single clonal populations in the lung have been shown to develop sub-clones within weeks of establishment,[5] and because cell lines and living tumors are known to gain resistance mutations over time, metastases with large proportions of cells with acquired resistance is a likely scenario in a patient, and the model likely reflects selection *in vivo*.

Qualitative comparisons can be made between prior data and model outcomes. Overall, the acquired resistance model produced rounds of cell death under drug concentrations in patients, showing that the parameters are biologically reasonable. The results are consistent with survival data for patients with inoperable locally advanced or metastatic bladder cancer undergoing a GC or MVAC regimen; those who had lung, liver, or bone metastases had a 5-year overall survival rate of 6.8%.[19] The likelihood of a patient presenting with a completely drug-sensitive metastatic population is low, creating low likelihood of complete cell killing in the tumor. Similarly, in the model, we saw only the most sensitive populations being eradicated by the standard regimen. A patient's metastatic population might have been completely sensitive if metastasis was recently established from a sensitive primary cell and lacked the time to gain genetic heterogeneity. Less likely still, several weeks or more after establishment, the metastases may have either not gained new genetic heterogeneity, or simply not acquired resistance through genetic aberrations. Finally, cells in the model had IC50s derived from cell lines, and some cells died at *in vivo* drug concentrations, suggesting that cell line data reasonably reflects the range of resistances found in patients' tumor cells. While these comparisons to patients and cells are speculative, they are valuable observations for generating hypotheses and represent opportunities for empirical validation as we develop the model further.

When acquisition of resistance was removed, some cells that had initial resistance survived and propagated. This "resistance" occurred because accumulated drug was divided in half between offspring, giving both sensitive and resistant primary sub-clones more time to grow and replicate before reaching IC50, with proliferation outpacing the delivery of drug. This result, in which cells randomly evade death without incorporating new resistance mechanisms, emphasizes the importance of considering growth rate in an aggressive metastatic population.

To estimate the number of doses required to actually kill a metastasis, we simulated delivery of gemcitabine every 24 hours over 126 days, along with synergistic cisplatin every 21 days. Even this unrealistic regimen did not kill the tumor, and drove it to gain cisplatin resistance. Increasing gemcitabine dosage, in combination with increasing the frequency of cisplatin at lower doses should be explored in the future. Additionally, drug regimens that incorporate other drugs besides cisplatin and gemcitabine will be explored in future iterations of the model.

There are caveats to this approach that we must consider. Our model is small (20×20×1 cells) for relatively fast computation so that many scenarios could be explored. Although this size still allowed differential effects to emerge between different drug scenarios, and computational costs scaled proportionally to the number of cells during growth from 100 to 400 cells, larger grids will be part of future work, hopefully approaching the clinical detection limit for lung metastases. The system modeled is specific to bladder cancer; however, lung is a common metastatic site for many other cancers. This and the available data on vascularity at urogenital metastatic sites helped justify the choice of the system modeled. Additionally, the model is simple and general, in part because a GC regimen is used in a variety of cancers, and can be relatively easily adapted to other metastatic or primary sites by replacing parameters in the code. The primary bottleneck to adaptation to other cancers will be the availability of empirical data to derive model parameters.

The model may be allowing consistent tumor survival despite an aggressive drug regimen due to a cell cycle time of 30h +/-1h (S.D.); slower- (or even faster-) cycling cells may create different dynamics. Drug is not delivered from vessels outside of the tumor, inherent cell death rates are not included, and the immune system is not directly considered. Most importantly, although the model can be manipulated unrealistically, useful hypothetical regimens must include practical considerations for regimens given to patients. If a new regimen kills more cells, perhaps the immune system will have a greater chance to reduce a smaller residual population. A simple increase in cell kill under an organizational and dosing scheme reasonable for patients is therefore a goal for this modeling process and the subject of future studies.

Finally, our model results recapitulate prior work by Powathil *et al.*[15] regarding the importance of accounting for cell cycle in drug delivery. Also our results concur with aspects of Waclaw *et al.*,[41] showing that after cell kill opens up space in the tumor, it takes only one or two cells to repopulate the vacant area with a new more resistant sub-clone. Such cell behavior is extremely difficult to track through time in a patient, and even in experimental models such as mice. Therefore, the importance of spatiotemporal models incorporating realistic parameters, with behavior that can be tracked over time to clinically relevant outcomes, cannot be underestimated.

Acknowledgments

References

1. Saunders, N. A. *et al. EMBO Mol. Med.* **4,** 675–84 (2012).
2. Tabassum, D. P. & Polyak, K. *Nat. Publ. Gr.* **15,** 1–11 (2015).
3. Yamamoto, N. *et al. Cancer Res.* **63,** 7785–90 (2003).
4. Talmadge, J. E. & Zbar, B. *J Natl Cancer Inst* **78,** 315–320 (1987).
5. Poste, G. *et al. Proc. Natl. Acad. Sci. U. S. A.* **79,** 6574–8 (1982).
6. Burrell, R. A. *et al. Mol. Oncol.* **8,** 1095–111 (2014).
7. Andasari, V. *et al. J. Math. Biol.* 1-31–31 (2010).
8. Mansury, Y. *et al. J. Theor. Biol.* **219,** 343–370 (2002).
9. Martins, M. L. *et al. Phys. Life Rev.* **4,** 128–156 (2007).
10. Powathil, G. G. *et al. J. Theor. Biol.* **401,** 1–14 (2016).
11. Tracqui, P. *et al. Cell Prolif.* **28,** 17–31 (1995).
12. Stamatakos, G. & Antipas, V. *IEEE Trans.* (2006).
13. Mansury, Y. *et al. J. Theor. Biol.* **238,** 146–156 (2006).
14. De La Cruz, R. *et al.* arXiv:1607.01449v1 (2016).
15. Powathil, G. G. *et al. Semin. Cancer Biol.* **30,** 13–20 (2015).
16. Siegel, R. L. *et al. CA. Cancer J. Clin.* **66,** 7–30 (2016).
17. Piergentili, R. *et al. Curr. Med. Chem.* **21,** 2219 (2014).
18. Sternberg, C. N. *Ann. Oncol.* **17,** 23–30 (2006).
19. von der Maase, H. *et al. J. Clin. Oncol.* **23,** 4602–4608 (2005).
20. National Comprehensive Cancer Network. Bladder Cancer v.1.2016, accessed 5/3/2016
21. Johnstone, T. C. *et al. Philos. Trans. A. Math. Phys. Eng. Sci.* **373,** (2015).
22. van Moorsel, C. J. *et al. Br. J. Cancer* **80,** 981–90 (1999).
23. Mistry, P. *et al. Cancer Res.* **52,** 6188–6193 (1992).
24. Henderson, P. T. *et al. Int. J. cancer* **129,** 1425–34 (2011).
25. Torres, M. P. *et al. PLoS One* **8,** e80580 (2013).
26. Kim, E. S. *et al. J. Clin. Oncol.* **30,** 3345–52 (2012).
27. Moufarij, M. *et al. Mol. Pharmacol.* **63,** 862–9 (2003).
28. Besançon, O. G. *et al. Cancer Lett.* **319,** 23–30 (2012).
29. Sandler, A. B. *et al. J. Clin. Oncol.* **18,** 122–130 (2000).
30. Fukata, S. *et al. Cancer* **103,** 931–942 (2005).
31. Papadopoulos I. *et al. J. Clin. Pathol.* **57,** 250 (2004).
32. Swat, M. H. *et al. Methods Cell Biol.* **110,** 325–66 (2012).
33. Kanigel Winner, K. *et al. Cancer Res.* 0008-5472.CAN-15-1620- (2015).
34. Yang, W. *et al. Nucleic Acids Res.* **41,** D955-61 (2013).
35. Vallo, S. *et al. Transl. Oncol.* **8,** 210–216 (2015).
36. Damaraju, S. *et al. Biochem. Pharmacol.* **79,** 21–9 (2010).
37. Ning S. *et al. Int. J. Oncol.* (2004).
38. Grunewald, R. *et al. Cancer Chemother. and Pharmacol.* **27,** 258 (1990).
39. Köberle, B. & Piee-Staffa, A. *Bladder Cancer - From Basic Science to Robotic Surgery.* **Chapter 13**, 265 (2012).
40. Nugent, L. J. & Jain, R. K. *Cancer Res.* **44,** 238–244 (1984).
41. Waclaw, B. *et al. Nature* **525,** 261–264 (2015).
42. Gilloteaux, J. *et al. Anat. Rec. A. Discov. Mol. Cell. Evol. Biol.* **288,** 58–83 (2006).
43. Wagner, B. J. *et al. J. Cell. Sci.* **124,**1644 (2011).
44. Koberle, B. *et al. Biochem. Pharmacol.* **52,** 1729–1734 (1996).
45. Fan, Y. *et al. Acta Pharmacol. Sin.* **31,** 746–52 (2010).
46. De Jongh, F. E. *et al. J. Clin. Oncol.* **19,** 3733–3739 (2001).